Triggering in thermoacoustics

Matthew P. Juniper*

Under certain conditions, the flow in a combustion chamber can sustain large amplitude oscillations even when its steady state is linearly stable. Experimental studies show that these large oscillations can sometimes be triggered by very low levels of background noise. This theoretical paper sets out the conditions that are necessary for triggering to occur. It uses a weakly nonlinear analysis to show when these conditions will be satisfied if the heat release rate is a function of the acoustic velocity amplitude. The role played by non-normality is investigated. It is shown that, when a state triggers to sustained oscillations from the lowest possible energy, it exploits transient energy growth around an unstable limit cycle. The positions of these limit cycles in state space is determined by nonlinearity, but the tangled-ness of trajectories in state space is determined by non-normality. When viewed in this dynamical systems framework, triggering in thermoacoustics is seen to be directly analogous to bypass transition to turbulence in pipe flow.

Nomenclature

Roman

a_s	a steady state amplitude
c_v	the constant volume specific heat capacity
c_0	the speed of sound within the acoustic duct
$h(\eta, \dot{\eta})$	a generic nonlinear function of η and $\dot{\eta}$
$\mathbf{I}$	the identity matrix
L_0	the length of the acoustic duct
M	the Mach number
$\mathbf{M}$	the monodromy matrix
n	an integer
p	the acoustic pressure perturbation within the acoustic duct
p_0	the unperturbed pressure within the acoustic duct
P	a generic control parameter
P_l	the value of the control parameter above which the system is linearly unstable
P_c	the value of the control parameter below which no periodic solutions exist
$\tilde{\dot{Q}}$	the heat transfer to the gas within the acoustic duct
q	the reduced heat transfer: $2\pi\tilde{\dot{Q}}(\gamma-1)/(\gamma p_0 u_0)\sin x_f$
q_1	$(\mathrm{d}q/\mathrm{d}\eta)$ evaluated at $\eta = 0$
q_2	$(\mathrm{d}^2q/\mathrm{d}\eta^2)/2!$ evaluated at $\eta = 0$
q_3	$(\mathrm{d}^3q/\mathrm{d}\eta^3)/3!$ evaluated at $\eta = 0$
r	the amplitude of η_0
R	the gas constant
S	the resolvent norm: $\|\|(\mathrm{i}\omega\mathbf{I} - \mathbf{M})\|\|^2$
T	the long timescale
T_0	the unperturbed temperature within the acoustic duct
u	the acoustic velocity perturbation within the acoustic duct
u_0	the unperturbed velocity within the acoustic duct
x_f	the flame or hot wire position

Greek

*Senior lecturer, Engineering Department, Trumpington Street, Cambridge, CB2 1PZ, United Kingdom.

γ the ratio of the specific heat capacities
δ the Dirac delta
ϵ a small parameter
ζ the acoustic damping
η the amplitude of the acoustic velocity perturbation, u
η_0 the contribution to η at order 1
η_1 the contribution to η at order ϵ
$\dot{\eta}$ $\mathrm{d}\eta/\mathrm{d}t$
λ the time delay between a velocity perturbation, u, and the correponding heat release perturbation, q
λ_t the thermal conductivity within the acoustic duct
ρ_0 the unperturbed density within the acoustic duct
τ the oscillation period, which is also the short timescale
ϕ the phase of η_0
ω the oscillation frequency of η_0
$||\cdot||$ the 2-norm

Superscript
$\tilde{}$ dimensional

Subscript
f at the flame or hot wire position
0 unperturbed

I. Introduction

Triggering was first observed in liquid and solid rocket motors in the 1960's.[1] Motors that seemed to be stable and quiet would jump to a self-sustained oscillating state when given a sufficiently large impulse. The same phenomenon has been seen in a model gas turbine engine[2] and in models of thermoacoustic systems.[3–5]

The first analyses of triggering were motivated by liquid rocket motors[6] and showed that some systems could sustain thermoacoustic oscillations even when they were linearly stable. In rocket engines, the oscillations have sufficiently high amplitude that the gas dynamics are nonlinear. Perhaps for this reason, most early studies of triggering assumed nonlinear gas dynamics but retained linear combustion models.[7–14] They concluded that nonlinear gas dynamics, even up to third order, cannot explain triggering.[15]

Later studies[3,17,18] included nonlinear combustion. The nonlinearities in these studies took two forms: (1) nonlinearities arising from quadratic terms in the fluctuating velocity, u, and fluctuating pressure, p, such as u^2; (2) a nonlinearity arising from a modulus sign, such as $|u|$. These studies showed that triggering can be achieved when the combustion is nonlinear and they explored the types of nonlinear models that give rise to experimentally-observed behaviour.

More recently, research into thermoacoustic instability has mainly been motivated by gas turbine engines.[16] The energy density inside a gas turbine is considerably less than that inside a rocket engine. This means that the thermoacoustic oscillations have lower amplitude and are usually sufficiently small that nonlinear gas dynamics can be neglected. It is also worth mentioning that, in gas turbines, the heat release fluctuations tend to be a function of the velocity fluctuations (velocity-coupling) rather than the pressure fluctuations (pressure-coupling).

Given that triggering seems to be particularly influenced by nonlinear combustion but not by nonlinear gas dynamics, this paper is restricted to linear gas dynamics and nonlinear combustion. It is also restricted to velocity-coupling, although the extension to pressure-coupling is simple.

Previous papers have usually examined combustion models in which the heat release fluctuations are a quadratic or cubic function of the acoustic velocity or pressure fluctuations. The first sections of this paper (§II – §IV), however, do not place any restriction on the nonlinear relationship between velocity and heat release. This produces a simple criterion for the type of system in which triggering is possible. Any velocity-coupled combustion model can be tested against this criterion by evaluating the first, second and third derivatives of heat release with respect to velocity around the steady state.

In a system that can have several different oscillating states, it is possible to switch from one oscillating state to another, either with an external pulse, or spontaneously.[19] In this paper, this type of transition will be called *mode switching*, and the word *triggering* will be reserved for the special case when the system

transitions from a stationary state to an oscillating state.

The aims of this paper are to set the context of triggering by describing supercritical and subcritical bifurcations (§II), to outline the conditions required for triggering (§III) and derive a necessary criteria for triggering in terms of the velocity-coupling (§IV), to explain why systems can trigger when pulsed at moderate amplitudes (§V), to show how non-normality can cause systems to trigger when pulsed at small amplitudes (§VI), to describe how to identify the smallest amplitude that causes triggering (§VII), and to show that triggering in thermoacoustics is analogous to bypass transition to turbulence (§VIII). The scope of this paper is to examine simple systems from a theoretical point of view, in order to explain the principles of triggering rather than to give accurate predictions of experimental results. The analysis in this paper has been adapted from the fields of optimal control, nonlinear dynamical systems, and hydrodynamics.

II. Bifurcation Diagrams

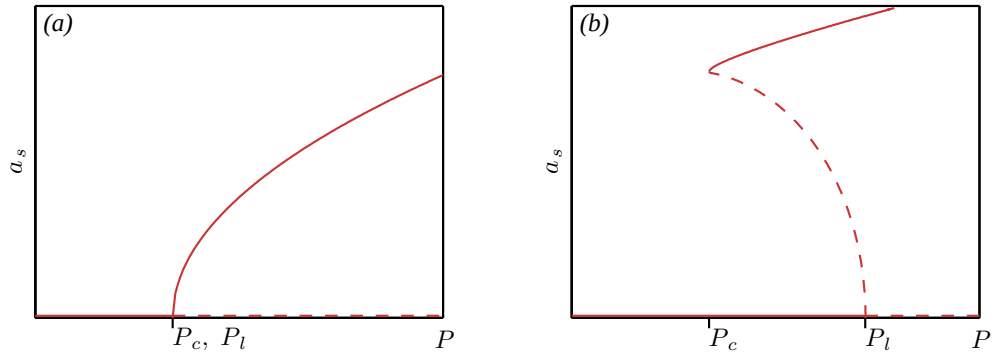

Figure 1. The steady state oscillation amplitude, a_S, as a function of a control parameter, P, for (a) a supercritical bifurcation and (b) a subcritical bifurcation. P_l is the point at which the fixed point (*i.e.* the zero amplitude solution) becomes unstable. P_c is the point below which no oscillations can be sustained.

Two systems with the same control parameter, P, are shown in figure 1. Some measure of the steady state amplitude of the system, a_S, is plotted on the vertical axis. In an oscillating system, this is often the peak-to-peak amplitude of the oscillations. There is a solution with zero amplitude, which is called a fixed point. At low values of P, on the left of figures 1(a,b), the fixed point is stable. When P reaches the Hopf bifurcation point, which is at P_l, this fixed point becomes unstable. The system starts to oscillate and eventually reaches the steady state amplitude given by the solid line. This state of the system is called a periodic solution, or limit cycle.

The nonlinear behaviour around the Hopf bifurcation point at P_l defines which type of bifurcation it is. The first type is a supercritical bifurcation (figure 1a) and is characterized by an amplitude that grows gradually with P for $P > P_l$. The second type is a subcritical bifurcation (figure 1b) and is characterized by an amplitude that grows suddenly as P increases through P_l. The second type has two stable solutions for $P_c \leq P \leq P_l$.

Periodic solutions are not the only possible solutions to nonlinear differential equations. There can also be multi-periodic, quasi-periodic and chaotic solutions, as described in textbooks on nonlinear dynamics.[20] These types of solution appear in thermoacoustic models[21] and in thermoacoustic experiments[22] but are beyond the scope of this paper.

III. Necessary criteria for triggering

In order for triggering to be possible, the thermoacoustic system must have operating points that can support a stable fixed point and another stable attractor (the second attractor does not have to be periodic). The simplest system that can exhibit triggering has a subcritical Hopf bifurcation to an unstable periodic solution (at P_l in figure 1b), followed by a fold bifurcation to a stable periodic solution (at P_c in figure 1b). This type of system will be examined in this paper because it is simple.

Systems with different types of bifurcations can also exhibit triggering. One example is a system with a supercritical Hopf bifurcation to a stable periodic solution, followed by a fold bifurcation to an unstable

periodic solution, followed by another fold bifurcation to a stable periodic solution, as shown in figure 2(b) of Ananthkrishnan *et al.*.[18] Other examples are systems with a stable fixed point and a multi-periodic, quasi-periodic or chaotic attractor. These system can trigger to sustained oscillations but these do not have a simple period. It is important to bear in mind that the existence of a stable periodic solution is not a necessary condition for triggering. In early papers, which were written before nonlinear dynamics and chaos were widely known, the existence of a periodic solution was thought to be necessary.

The most complete way to identify systems that can exhibit triggering is to map the bifurcation diagram as a function of the control parameters. Recent work[23] has shown that this is straightforward for network models[24] with simple heat release models. It is also relatively easy for thermoacoustic systems whose heat release has been characterized by a Flame Describing Function (FDF).[19] The FDF quantifies how the amplitude and phase of the heat release fluctuations vary with the amplitude and frequency of the velocity fluctuations.

The type of Hopf bifurcation can be determined, however, without mapping the bifurcation diagram. The technique described in §IV determines this from the amplitude of small heat release fluctuations as a function of the amplitude of small velocity fluctuations. This quickly indicates whether a system is susceptible to triggering. A complete analysis, including the phase variation, is more difficult and will be presented in another paper.

For systems that simulate the acoustics and heat release simultaneously, without encapsulating the interaction in an FDF,[4,5] it can take a long time to map the bifurcation diagram. Nevertheless, this approach is already feasible[26,27] and with improvements in continuation methods and the application of parallel computing, continuation methods are likely to become important tools in nonlinear analysis of thermoacoustics.

IV. Weakly nonlinear analysis around the Hopf bifurcation point

A weakly nonlinear analysis can determine the nature of a Hopf bifurcation point. This method has been performed before on thermoacoustic systems[6] and makes similar assumptions to the time averaging approach in many of Culick's papers.[11] The process in this paper differs from that in previous papers, however, due to the Maclaurin expansion (7), which allows the method to be applied to any velocity-coupled heat release model.

The thermoacoustic system examined in this paper is a tube of length L_0 in which a velocity-coupled compact heat source is placed distance $\tilde{x}_f$ from one end.[4,26] A base flow is imposed through the tube with velocity u_0. The physical properties of the gas in the tube are described by c_v, γ, R and λ_t, which represent the constant volume specific heat capacity, the ratio of specific heats, the gas constant and the thermal conductivity respectively. The unperturbed quantities of the base flow are ρ_0, p_0 and T_0, which represent density, pressure and temperature respectively. From these one can derive the speed of sound $c_0 \equiv \sqrt{\gamma R T_0}$ and the Mach number of the flow $M \equiv u_0/c_0$.

Acoustic perturbations are considered on top of this base flow. In dimensional form, the perturbation velocity and perturbation pressure are represented by $\tilde{u}$ and $\tilde{p}$. Quantities evaluated at the flame's position, $\tilde{x}_f$, have subscript f. The rate of heat transfer to the gas there is given by $\tilde{\dot{Q}}$, which depends on u in a way that will be defined later. Acoustic damping is represented by ζ.

The dimensional momentum and energy equations for the acoustic perturbations are:

$$\rho_0 \frac{\partial \tilde{u}}{\partial \tilde{t}} + \frac{\partial \tilde{p}}{\partial \tilde{x}} = 0, \tag{1}$$

$$\frac{\partial \tilde{p}}{\partial \tilde{t}} + \gamma p_0 \frac{\partial \tilde{u}}{\partial \tilde{x}} + \zeta \frac{c_0}{L_0} \tilde{p} - (\gamma - 1) \tilde{\dot{Q}} \tilde{\delta}(\tilde{x} - \tilde{x}_f) = 0. \tag{2}$$

Reference scales for speed, pressure, length and time are u_0, $p_0 \gamma M$, L_0 and L_0/c_0. The dimensional variables, coordinates and Dirac delta can then be written as:

$$\tilde{u} = u_0 u, \quad \tilde{p} = p_0 \gamma M p, \quad \tilde{x} = L_0 x \quad \tilde{t} = (L_0/c_0) t, \quad \tilde{\delta}(\tilde{x} - \tilde{x}_f) = \delta(x - x_f)/L_0, \tag{3}$$

where the quantities without a tilde or subscript 0 are dimensionless. Substituting (3) into the dimensional governing equations (1) and (2) and making use of the definition of c_0 and the ideal gas law, $p_0 = \rho_0 R T_0$, gives the dimensionless governing equations for acoustic perturbations:

$$\frac{\partial u}{\partial t} + \frac{\partial p}{\partial x} = 0, \tag{4}$$

$$\frac{\partial p}{\partial t} + \frac{\partial u}{\partial x} + \zeta p - \frac{\gamma - 1}{\gamma p_0 u_0} \tilde{\dot{Q}} \delta(x - x_f) = 0, \tag{5}$$

The pipe has open ends at $x = 0$ and $x = 1$, at which $p = 0$ and $\partial u/\partial x = 0$. Only the first acoustic mode will be considered here, for which $u(x,t) = \eta \cos(\pi x)$ and $p(x,t) = -(\dot{\eta}/\pi)\sin(\pi x)$. When the higher modes are included, the analysis becomes much more complicated (but not impossible). The same is true of FDF analyses, for which the standard procedure is to consider just the first mode or to assume that the amplitudes of the higher modes are fixed multiplies of that of the first mode.[19] As a side-effect, this makes the system less non-normal. The first mode is substituted into (4–5), which are then rearranged to give:

$$\ddot{\eta} + \pi^2 \eta + \zeta \dot{\eta} + q = 0. \tag{6}$$

where $q \equiv 2\pi \tilde{\dot{Q}}(\gamma - 1)/(\gamma p_0 u_0) \sin x_f$. Equation (6) is similar to equation (46) in Culick[8] but with a simpler damping term and a general heat release term.

The heat release is taken to be a nonlinear function of the velocity magnitude, η, with a time delay, λ. This is a common assumption for the analysis of thermoacoustic systems that are representative of gas turbines. For further analysis, one of two assumptions must be made: (1) that the time delay, λ, is small compared with the oscillation period, τ, or (2) that η is periodic in t. The first assumption is chosen here because it does not preclude the non-periodic behaviour described later. This is reasonable when the heat release is from a heat source that reacts quickly to velocity changes, such as a hot thin wire, but not reasonable when the heat release is from a flame. It will be shown later that this analysis also requires the damping to be very small, which is satisfied in most thermoacoustic systems. With this assumption, the time-delayed heat release term can be approximated by $q(\eta(t - \lambda)) \approx q(\eta - \lambda\dot{\eta})$.

In a moment, a weakly nonlinear analysis around the Hopf bifurcation point will be performed, for which oscillations in q are small. In this case it is valid to take the Maclaurin expansion of q:

$$q(\eta(t-\lambda)) \approx q_1 \times (\eta - \lambda\dot{\eta}) + q_2 \times (\eta - \lambda\dot{\eta})^2 + q_3 \times (\eta - \lambda\dot{\eta})^3 + \ldots, \tag{7}$$

where $q_1 \equiv q'(0)$, $q_2 \equiv q''(0)/2!$ and $q_3 \equiv q'''(0)/3!$. For the weakly nonlinear analysis, this expansion is more general than assuming that q is a specified function of η, as in Refs.[3,6,8,10–15,18] Indeed, q_1, q_2, and q_3 can be extracted from any velocity-coupled heat release model, from an FDF, or from experimental data. In this paper, q will be expanded only to third order because this is the lowest order that determines the behaviour around the Hopf bifurcation point. Equation (7) is substituted into (6), which is re-arranged to give:

$$\ddot{\eta} + (\pi^2 + q_1)\eta + (\zeta - \lambda q_1)\dot{\eta} + q_2(\eta - \lambda\dot{\eta})^2 + q_3(\eta - \lambda\dot{\eta})^3 = 0. \tag{8}$$

The first two terms are those of a linear harmonic oscillator with angular frequency $(\pi^2 + q_1)^{1/2}$. (The shift in frequency due to heat release was noted by Rayleigh[25] pp. 226-227.) The third term represents the first order competition between heat release and damping. Around the Hopf bifurcation point, where the linear stability switches, this term is small because $(\zeta - \lambda q_1)$ changes sign there. When the amplitudes of η and $\dot{\eta}$ are also small, the final three terms are all much smaller than the first two terms and equation (8) can be put in the form:

$$\ddot{\eta} + (\pi^2 + q_1)\eta + \epsilon h(\eta, \dot{\eta}) = 0, \tag{9}$$

where ϵ is a small parameter and h is a generic nonlinear function of η and $\dot{\eta}$. If ϵ were zero, the solution to (9) would be a harmonic oscillation with constant amplitude and constant period. When ϵ is small, the solution to (9) is a similar harmonic oscillation with a similar period. The effect of the small term is to vary the amplitude and phase of this oscillation on a timescale that is order $1/\epsilon$ longer than the period. This makes the system susceptible to a two-timing analysis,[20] which is also known as a Van der Pol analysis.

In a two-timing analysis, a fast time, τ, and a slow time, T, are defined such that $\tau = t$ and $T = \epsilon t$. These variables, T and τ, are treated as if they are independent. The variable η is then expressed as a function of τ, T, and ϵ. The variables $\dot{\eta}$ and $\ddot{\eta}$ are evaluated using the chain rule:

$$\eta(\tau, T, \epsilon) = \eta_0(\tau, T) + \epsilon\eta_1(\tau, T) + \mathcal{O}(\epsilon^2) \tag{10}$$

$$\dot{\eta} = \frac{\partial \eta_0}{\partial \tau} + \epsilon\left(\frac{\partial \eta_1}{\partial \tau} + \frac{\partial \eta_0}{\partial T}\right) + \mathcal{O}(\epsilon^2) \tag{11}$$

$$\ddot{\eta} = \frac{\partial^2 \eta_0}{\partial \tau^2} + \epsilon\left(\frac{\partial^2 \eta_1}{\partial \tau^2} + 2\frac{\partial^2 \eta_0}{\partial \tau \partial T}\right) + \mathcal{O}(\epsilon^2). \tag{12}$$

Equations (10 – 12) are substituted into (8) and equated at different orders of ϵ. At $\mathcal{O}(\epsilon^0)$ and $\mathcal{O}(\epsilon^1)$ respectively they are:

$$\frac{\partial^2\eta_0}{\partial\tau^2} + (\pi^2 + q_1)\eta_0 = 0, \quad (13)$$

$$\frac{\partial^2\eta_1}{\partial\tau^2} + 2\frac{\partial^2\eta_0}{\partial T\partial\tau} + (\pi^2+q_1)\eta_1 + (\zeta - \lambda q_1)\frac{\partial\eta_0}{\partial\tau} + q_2\left(\eta_0 - \lambda\frac{\partial\eta_0}{\partial\tau}\right)^2 + q_3\left(\eta_0 - \lambda\frac{\partial\eta_0}{\partial\tau}\right)^3 = 0. \quad (14)$$

If variations of η_0 in the slow timescale, T, are frozen then equation (13) collapses to an O.D.E with solution

$$\eta_0 = r\cos(\omega\tau + \phi), \quad (15)$$

where $\omega^2 = (\pi^2 + q_1)$ and the amplitude, r, and phase, ϕ, are functions of the slow time, T. This behaviour was anticipated earlier from inspection of (9). In order to calculate the evolution of r and ϕ on the slow time, equation (15) is substituted into (14), which is re-arranged using trigonometric relations to give an inhomogenous O.D.E for η_1:

$$\begin{aligned}\frac{\mathrm{d}^2\eta_1}{\mathrm{d}\tau^2} + \omega^2\eta_1 &= \left[2\omega r\frac{\mathrm{d}\phi}{\mathrm{d}T} - q_3\frac{3(1+\lambda^2\omega^2)}{4}r^3\right]\cos(\omega\tau+\phi)\ldots \\ &+ \left[2\omega\frac{\mathrm{d}r}{\mathrm{d}T} + (\zeta - \lambda q_1)\omega r - q_3\frac{3\tau\omega(1+\tau^2\omega^2)}{4}r^3\right]\sin(\omega\tau+\phi)\ldots \\ &+ \text{ terms in } \cos n(\omega\tau+\phi) \text{ and } \sin n(\omega\tau+\phi) \text{ where } n \neq 1. \quad (16)\end{aligned}$$

The left hand side of (16) represents a linear oscillator with natural frequency ω. The terms in square brackets on the right hand side represent forcing exactly at this natural frequency. These terms, which are called secular terms, must be zero or they would result in unbounded growth and violate the assumption in (10) that the x_1 term is small. This means that either $r = 0$ or the amplitude and phase of the oscillations must vary on the slow timescale T according to:

$$\frac{\mathrm{d}r}{\mathrm{d}T} = \frac{(\lambda q_1 - \zeta)}{2}r + \frac{3\tau(1+\tau^2\omega^2))}{8}q_3r^3 \quad (17)$$

$$\frac{\mathrm{d}\phi}{\mathrm{d}T} = \frac{3(1+\lambda^2\omega^2)}{8\omega}q_3r^2. \quad (18)$$

There is a periodic solution if $\mathrm{d}r/\mathrm{d}T = 0$, which occurs when

$$r = \pm\left(\frac{4(\zeta - \lambda q_1)}{3q_3\lambda(1+\lambda^2\omega^2)}\right)^{1/2}. \quad (19)$$

For a damped system that can become linearly unstable, q_1 must be positive. The first term on the RHS of (17) represents linear driving if $\lambda q_1 > \zeta$ and the second term represents either cubic saturation if q_3 is negative, or cubic enhancement if q_3 is positive. This means that (19) has two types of solution, as shown in figure 2. If q_3 is negative, oscillations to the right of the Hopf bifurcation point are saturated by the cubic terms and the bifurcation is supercritical. If q_3 is positive, oscillations to the left of the Hopf bifurcation point are enhanced by the cubic terms and the bifurcation is subcritical. The same result can be derived with a time-averaging approach. For the square root nonlinearity in King's law, which is used in the Rijke tube model of the rest of this paper,[4,26] it is easy to show that q_3 is positive and therefore that the Hopf bifurcation is subcritical.

It is worth noting that this analysis requires the damping, ζ, to be very small if the frequency shift due to heat release is small. The latter assumption requires that $q_1 \ll \pi^2$, which means that $\tau \approx 2$. Around the Hopf bifurcation point, $\lambda \approx \zeta/q_1$, which means that $\lambda/\tau \approx \zeta/(2q_1)$. The two-timing analysis assumes that $\lambda/\tau \ll 1$, which means that $\zeta/(2q_1) \ll 1$ and, because q_1 is small, means that ζ is very small. Fortunately for this analysis, thermoacoustic systems are prone to instability precisely because their acoustic damping is very small.

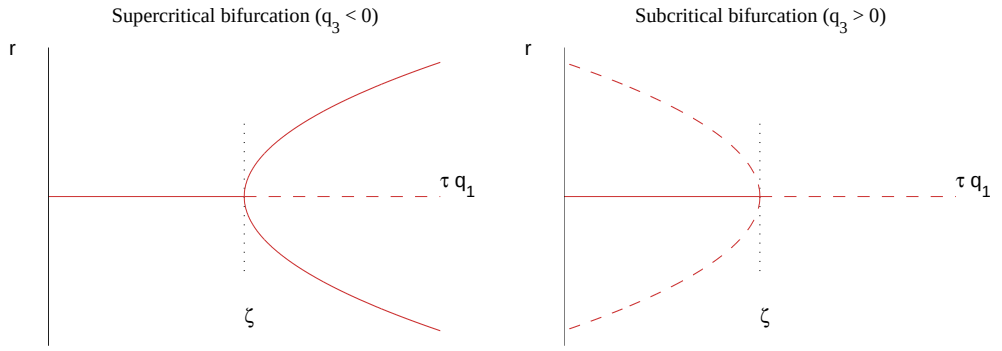

Figure 2. Periodic solutions predicted from the weakly-nonlinear analysis around the Hopf bifurcation point. Solid lines are stable solutions. Dashed lines are unstable solutions. When q_1 is positive, the type of Hopf bifurcation depends on the sign of q_3 in (19). When q_3 is negative (left), cubic terms are saturating and the bifurcation is supercritical. When q_3 is positive (right), cubic terms are enhancing and the bifurcation is subcritical. q_1 and q_3 are the first and third derivatives of $q(\eta)$ in the Maclaurin series (7).

V. Triggering

The evolution of the single mode system considered in section IV can be described in terms of the oscillation amplitude, r, and phase, ϕ. If the system has a subcritical bifurcation ($q_3 > 0$) then equation (17) shows that, if the amplitude, r, increases above that of the unstable limit cycle, then it must continue to grow.

For the single mode system, this gives a simple criterion for the onset of triggering: the amplitude must exceed that of the unstable periodic solution. This is true for single mode systems and systems that are modelled in terms of the amplitude of a single mode. For instance, Noiray *et al.*[19] evaluated the nonlinear Flame Describing Function (FDF) of a laboratory burner with multiple flames and used it to create the bifurcation diagram, which had stable and unstable periodic solutions. They considered the amplitude and phase of only the fundamental mode and assumed that the higher harmonics were locked to this mode. Then they numerically evaluated trajectories in state space and showed that mode-switching occurs when the amplitude tips to one side or the other of an unstable periodic solution (their Figure 9a). Finally, they compared their results with experimental measurements, which showed that mode switching occurs when the amplitude passes that of the unstable periodic solution. (This can be seen by comparing their figure 17 with their figure 12). This is a remarkably successful experimental demonstration of the role of unstable periodic solutions in mode-switching.

Experiments on a ducted flame[28] and an electrically-heated Rijke tube[29] show similar behaviour. In these experiments, the bi-stable region of the systems was evaluated (this is the region where a stable fixed point co-exists with a stable periodic solution) and the frequency of the stable periodic solution was measured. Then the systems were set to the non-oscillating state and forced briefly at the frequency of the stable periodic solution. The forcing was either for a prescribed number of cycles at a variable amplitude or for a variable number of cycles at a prescribed amplitude. The forcing caused the amplitude of the system to grow until the forcing was switched off. After that, it either decayed back to the fixed point, or grew on to the stable periodic solution. In this way, the triggering threshold was identified. These experiments also showed that, just above the threshold, the amplitude grew very slowly. This is consistent with the threshold being the unstable periodic solution although, unlike Noiray *et al*,[19] they did not evaluate the Flame Describing Function and therefore could not calculate the unstable periodic solution with a frequency domain stability analysis.

The studies described above were all on systems that have dominant periodic solutions at isolated frequencies. Mode switching and triggering were examined either when the system was oscillating at these frequencies[19] or when the system was forced at these frequencies.[28,29] In all cases, the amplitude grew relatively slowly and was not suddenly increased by a pulse.

Wicker *et al.*[3] examined the triggering behaviour when a two-mode system was pulsed suddenly. They found that the threshold amplitude for triggering varied significantly with the relative phases of the initial modes and varied slightly with their harmonic content. In particular, they found that, for triggering to occur, the initial amplitude of the first mode had to be greater than that of the second. This shows that,

in a system with more than one mode, there is more to triggering than simply increasing the amplitude of a pulse above a certain value. The type of pulse is also important.

On the one hand, this is easy to understand in terms of damping: different modes have different levels of damping and the system will not grow as strongly if one of its heavily-damped modes is pulsed than if one of its lightly-damped modes is pulsed. This can be seen clearly in Waugh *et al.*,[30] which shows the behaviour of a ten-mode thermoacoustic system when triggered from twenty different initial pulses. These pulses were chosen because they all led (or nearly led) to triggering. The pulses that led to triggering from the lowest possible initial energy had most of their energy in the least-damped mode which, like the system of Wicker *et al.*,[3] was the first mode. The same argument can be applied in terms of the harmonic content of the unstable periodic solution: the unstable periodic solution, like the stable periodic solution, has most of its energy in the least damped mode, which in Wicker *et al.*'s case was the first mode. If a system is pulsed close to this unstable periodic solution, but with infinitesimally more energy, it will grow to the stable periodic solution. Therefore, to a first approximation, the pulse must also have most of its energy in the least damped mode.

On the other hand, some experiments have shown that triggering can be achieved with nothing more than background noise.[2] Although it is not possible to work out the unstable periodic solution from the reported results of these experiments, it is likely that its amplitude was significantly greater than the amplitude of the background noise. This is difficult to explain in terms of the reasoning in the previous paragraphs, and impossible to explain for a single mode system. A deeper explanation must include the role of non-normality in these systems (§VI), particularly around the unstable periodic solution.

VI. The role that non-normality plays in triggering

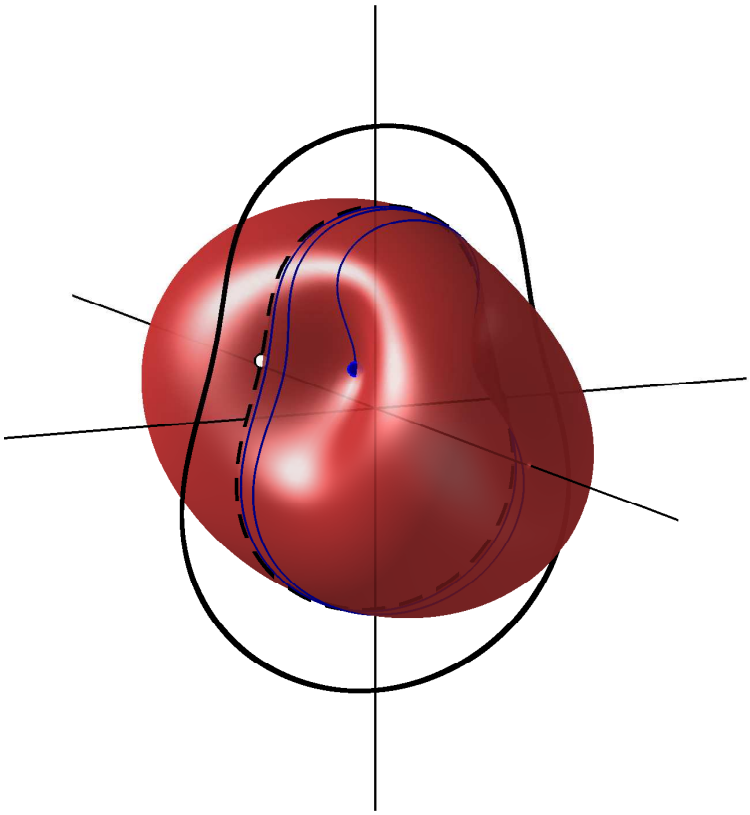

Figure 3. A cartoon of the manifold that separates the basin of attraction of the stable fixed point (at $(0, 0, 0)$, inside the manifold) from the basin of attraction of the stable periodic solution (the loop outside the manifold). The unstable periodic solution (dashed line) is a loop exactly on the manifold. All states exactly on the manifold are attracted to the unstable periodic solution (blue line).

In a thermoacoustic system, the acoustic energy is held alternately by the acoustic velocity and the acoustic pressure. If a thermoacoustic system is modelled by a single mode[8,19] then the corresponding dynamical system has two degrees of freedom: one for the amplitude of the acoustic velocity and one for the amplitude of the acoustic pressure. The state space for this model is a two-dimensional plane.

In the bi-stable regime of the single mode system (for which a stable fixed point and a stable periodic solution co-exist), the unstable and stable periodic solutions are both closed loops in state space. The stable fixed point lies within the unstable periodic solution and both of these lie within the stable periodic solution. Because lines in state space cannot cross, and because this state space is two-dimensional, all trajectories in state space that start outside the unstable periodic solution must end up on the stable periodic solution and all trajectories that start inside the unstable periodic solution must end up on the stable fixed point. Consequently, in a single mode system, the unstable periodic solution is the boundary of the basin of attraction of the stable periodic solution.

If the dynamical system has N degrees of freedom, the basin boundary is an $(N-1)$-dimensional manifold in N-dimensional space. It is difficult to visualise this basin boundary but a cartoon of a two-dimensional manifold in three-dimensional space is shown in figure 3 for illustration. (It is important to remember, however, that on a manifold with more than two dimensions, trajectories on the manifold can pass each other without intersecting.)

The red surface is the closed manifold that separates the states that evolve to the stable fixed point, which lies inside the surface, from the states that evolve to the stable periodic solution, which is the large loop that lies away from the surface. Points *exactly* on the manifold remain on the manifold for all time. Any state on this manifold, if given an infinitesimal increase in amplitude, would evolve to the stable periodic solution. The question of triggering therefore boils down to finding the lowest energy point on this manifold. The unstable periodic solution is a loop exactly on this manifold, so the lowest energy point on this loop is a good starting point. For multi-mode systems, the question is whether there are any points on this basin boundary with lower energy than this.

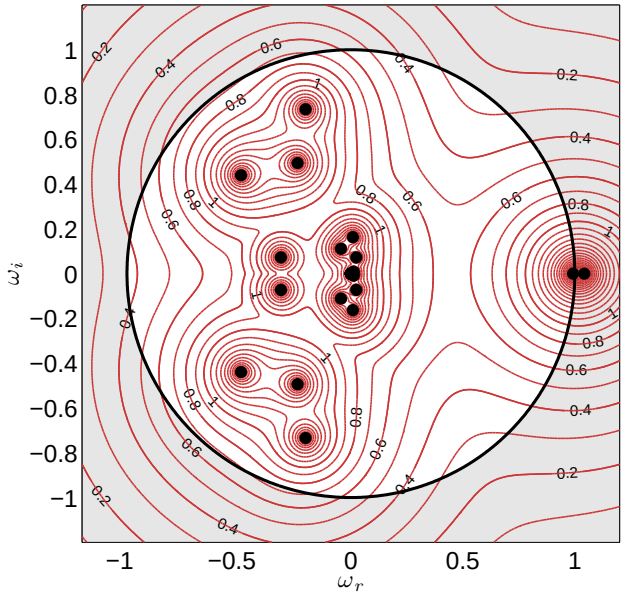

Figure 4. Eigenvalues (black dots) and pseudospectra (red lines) of the monodromy matrix, M. This matrix describes the evolution of an infinetismal perturbation after one loop around the unstable periodic solution of a dynamical system representing a 10 mode Rijke tube.[26] The thick black line is the unit circle. The eigenvalues, which are also known as the Floquet multipliers, are stable if they lie within the unit circle. Here, one is unstable, one is neutral and the rest are stable. The pseudospectra are shown here as $\log_{10}(S)$, where S is the resolvent norm: $S \equiv ||(\mathbf{i}\omega\mathbf{I} - \mathbf{M})||^2$. They extend slightly further out than they would if the system were normal, particularly around the three eigenvalues at highest ω_i. This implies that there will be some transient growth[31] although, with only slight non-normality, it will be small for this model.

Let us consider small perturbations around the unstable periodic solution. We do this by generating the monodromy matrix,[31] which maps the evolution of an infinitesimal perturbation after it has looped once around the periodic solution. The eigenvalues and pseudospectra of the monodromy matrix of a 10 mode Rijke tube[26] are shown in figure 4. For this system, there are eighteen eigenvalues inside the unit

circle, which are stable, one eigenvalue on the unit circle, which is neutrally stable and represents motion in the direction of the periodic solution, and one eigenvalue outside the unit circle, which is unstable. This shows that the unstable manifold attracts states from every direction except one. The pseudospectra are not quite concentric circles centred on the eigenvalues, which shows that the system is non-normal and therefore susceptible to transient growth.

Small perturbations exactly on the manifold stay on the manifold for all time and therefore have no component in the direction of the unstable eigenvalue. After many cycles, these perturbations are attracted towards the unstable periodic solution. At intermediate times, however, these perturbations can grow away from the unstable periodic solution. By inspecting the directions in which they grow,[26] it can be shown that trajectories on the manifold around the unstable periodic solution can have both higher or lower energy than the unstable periodic solution itself. Therefore, there are states on the manifold that grow transiently in energy before being attracted towards the unstable periodic solution. These are the states adjacent to the ones that trigger to the stable solution from the lowest energy. In other words, if one imagines trajectories in state space to be infinitely-long lines of spaghetti on the surface of the manifold, the role of non-normality is to tangle up the lines of spaghetti and send some of them to lower energies than would be expected without non-normality. The one that triggers from the lowest possible energy is called the *most dangerous* initial state. Having shown that it exists away from the unstable periodic solution, the next step is to devise a systematic way to find it.

VII. Finding states that trigger from the lowest possible energy

The state with maximum linear transient growth away from the stable fixed point is the first singular vector of the linear operator that governs the evolution of infinitesimal perturbations around the stable fixed point.[4,5,31] Similarly, the state with maximum linear transient growth around the unstable periodic solution is the first singular vector of the monodromy matrix described in §VI. These results only apply, however, to infinitesimal disturbances. In order to find the most dangerous initial state, a procedure must be developed that can handle disturbances of a finite size.

A convenient technique is adapted from optimal control.[32] A cost functional, $\mathcal{J}$, is defined as the ratio of final energy to initial energy over some time period, T. A Lagrangian functional, $\mathcal{L}$, is then defined as the cost functional, $\mathcal{J}$, minus a set of inner products. These inner products multiply the governing equations by one set of Lagrange multipliers and the initial state by another set of Lagrange multipliers. When all variations of $\mathcal{L}$ with respect to the Lagrange multipliers, state variables, $\mathbf{x}$, and initial state, $\mathbf{x}_0$, are zero then an initial state has been found that optimizes $\mathcal{J}$ and satisfies the governing equations.

To find this initial state, the direct governing equations are integrated forward for time T from an initial guess, thus satisfying the requirement that all variations of $\mathcal{L}$ with respect to the Lagrange multipliers are zero. The Lagrangian functional is then re-arranged so that it is expressed in terms of a different set of inner products. These inner products multiply the state variables, $\mathbf{x}$, by a first set of constraints. They also multiply the initial state, $\mathbf{x}_0$, by a second set of constraints. The requirement that all variations of $\mathcal{L}$ with respect to $\mathbf{x}$ are zero can be met by satisfying the first constraints. Half of these, known as the *optimality conditions* determine the relationship between an adjoint state vector, $\mathbf{x}^+$, and the direct state vector, $\mathbf{x}$, at time T. The other half, known as the *adjoint* governing equations, govern the evolution of $\mathbf{x}^+$ for $t = [0, T]$. After setting the optimality conditions at $t = T$, the adjoint governing equations are integrated backward to time 0, thus satisfying the requirement that all variations of $\mathcal{L}$ with respect to $\mathbf{x}$ are zero. The second set of constraints return the gradient information $\partial\mathcal{L}/\partial\mathbf{x_0}$ at the initial guess for $\mathbf{x}_0$. This is combined with a convenient optimization algorithm, such as the steepest descent method or the conjugate gradient method, in order to converge towards the optimal initial state, at which $\partial\mathcal{L}/\partial\mathbf{x_0} = 0$.

There are two ways to find the most dangerous initial state. The first is to use the knowledge that all states exactly on the manifold (figure 3) are attracted towards the unstable periodic solution. This means that the trajectory from the most dangerous initial state must pass infinitesimally close to the unstable periodic solution. A good starting point for the optimization procedure is therefore the lowest energy state on the unstable periodic solution. This technique was used in Ref.[26] Alternatively, the most dangerous initial state can be found by setting the optimization time, T, to be very large and starting from many hundred random initial states. This naturally finds states that reach the stable periodic solution from very low energies and avoids the criticism that the first technique might simply have found a local minimum. This technique was used in Refs.[33,34] Both techniques gave the same most dangerous initial state, which is

reassuring.

Figure 5 shows the evolution for the most dangerous initial state, taken from Ref.[26] There is strong transient growth in the first cycle, from an energy below the lowest energy on the unstable periodic solution. then the system settles towards the unstable periodic solution for many cycles before growing to the stable periodic solution, as expected.

The procedure in this section systematically finds the most dangerous initial condition and describes the system's evolution from that state. This is currently being extended to thermoacoustic systems with more realistic heat release models, which should trigger from lower initial energies because they have higher non-normality.

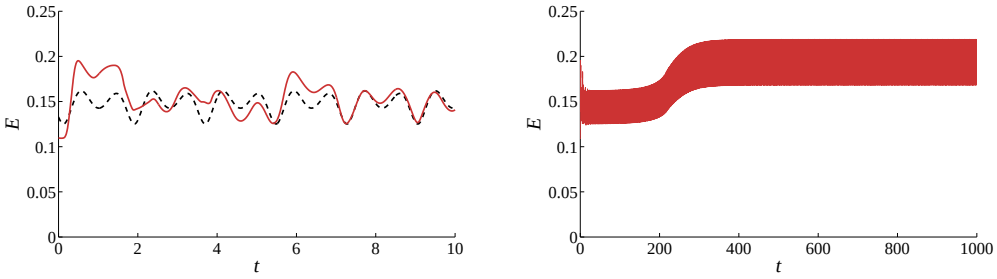

Figure 5. Evolution of the acoustic energy, E, as a function of time, T, starting from the most dangerous initial state (red line). The black dashed line shows the unstable periodic solution. Both frames show the same data on different timescales.)

VIII. The link with bypass transition to turbulence

Triggering in thermoacoustics is directly analogous to bypass transition to turbulence in hydrodynamics because both are examples of the evolution of trajectories around edge states in nonlinear dynamical systems. A fluid flow can be considered as a dynamical system with a very large number of degrees of freedom.[35–37] A boundary in state space can be identified between trajectories that decay to a laminar solution and trajectories that evolve to a turbulent solution. This boundary has become known as the *edge of chaos*[35] and it is directly analogous to the manifold shown in figure 3. This boundary contains several heteroclinic saddle points and at least one local relative attractor, each corresponding to a periodic travelling wave solution.[37] The state wanders from the vicinity of one travelling wave solution to the vicinity of another and so on until it reaches a local relative attractor, where it either evolves towards the laminar solution or to a turbulent solution. The local relative attractor in the hydrodynamic system is directly analogous to the unstable periodic solution in this paper's thermoacoustic system.

The role of non-normal transient growth is becoming increasingly apparent in hydrodynamic systems. For instance, the laminar flow in a round pipe becomes turbulent at a Reynolds number between 1,000 and 10,000 even though it is linearly stable at all Reynolds numbers. The likely mechanism is that small (but not infinitesimal) perturbations grow, due to non-normal transient growth, and then evolve to the turbulent solution due to the influence of the local relative attractor. In other words, in some of the many dimensions of the dynamical system, non-normality causes the edge of chaos to be extremely close to the stable fixed point. It seems likely that the same is true of thermoacoustic systems, which explains how they can sometimes trigger from low noise.

IX. Conclusions

One conclusion of this paper is that thermoacoustic systems should be considered as nonlinear dynamical systems and analysed with tools from that field. In nonlinear dynamical systems theory, the state of the system evolves along a trajectory in state space. Hidden amongst the possible trajectories there are some loops, which are the periodic solutions, and at least one point, which is the fixed point. (There may also be chaotic trajectories, but these have not been considered here.) All trajectories tend to the loops or the fixed point as time goes to positive or negative infinity. The positions of the loops and the point are determined only by the nonlinear characteristics of the system. They have nothing to do with non-normality. If the

system is normal, trajectories grow or decay monotonically around the periodic solutions and fixed point. If the system is non-normal, however, some trajectories can grow strongly away from the periodic solution or fixed point to which they ultimately decay. If the set of possible trajectories are thought of as lines of spaghetti in state space, then nonlinearity describes where they end up and where they started from, while non-normality describes how tangled they are.

Another conclusion concerns the relative importance of linear, nonlinear, and non-normal behaviour. The stability around the fixed point is the most important starting point and this is what would be called a conventional linear analysis. The next most important factor is the nature of the Hopf bifurcation, which can either be found with a weakly nonlinear analysis (§IV), with a continuation method, or with a Flame Describing Function. This determines whether the Hopf bifurcation is subcritical or supercritical. If it is subcritical, then triggering is possible. If it is supercritical then triggering is not certain, but may still be possible. (Higher order nonlinearities need to be considered in order to see whether there is a fold bifurcation to an unstable periodic solution.)

The fully nonlinear behaviour can be calculated with a continuation method. At the moment this is time-consuming, even for relatively small systems, but with faster algorithms and increased computing power, it may become feasible for larger systems. Continuation methods find fixed point and periodic solutions. Other solutions exist, such as multi-periodic, quasi-periodic, and chaotic solutions, but these are difficult to find with conventional continuation methods. The nonlinear periodic behaviour can also be estimated with an FDF analysis.

Once the nonlinear behaviour has been determined, one can consider the non-normal behaviour. If triggering is not possible (e.g. if the bifurcation is supercritical) then non-normality is little more than an interesting curiosity that makes a system more sensitive to noise. If triggering is possible, however, then the transient growth caused by non-normality provides a mechanism for a system to trigger, via the unstable periodic solution, from low amplitude initial pulses or low amplitude noise.[38] This helps to explain experimental results[2] concerning triggering and mode switching.

Acknowledgments

I would like to thank R.I.Sujith, Peter Schmid, Pankaj Wahi, Sathesh Mariappan, Priya Subramanian and Iain Waugh for helpful discussions during this work. It should be mentioned that Priya and Pankaj have independently done a weakly nonlinear analysis of the Rijke tube, published in Priya's thesis. This work was supported by the U.K. Engineering Physical and Sciences Research Council (EPSRC) and the AIM Network* through grants EP/G033803/1 and EP/GO37779/1.

References

[1]Culick, F. "Unsteady motions in Combustion Chambers for Propulsion Systems," *AGARD*, 2006, AG-AVT-039.

[2]Lieuwen, T. "Experimental investigation of limit-cycle oscillations in an unstable gas turbine combustor," *J. Prop. Power,* Vol. 18, No. 1, 2002, pp. 61–67.

[3]Wicker, J. M., Greene, W. D., Kim, S-I. and Yang, V. "Triggering of Longitudinal Pressure Oscillations in Combustion Chambers. I: Nonlinear Combustion Response" *J. Prop. Power,* Vol. 12 No. 6, 1996, pp. 1148–1158.

[4]Balasubramanian, K. and Sujith, R.I. "Thermoacoustic instability in a Rijke tube: nonnormality and nonlinearity" *Phys. Fluids* Vol. 20, 2008, 044103.

[5]Balasubramanian, K. and Sujith, R.I. "Non-normality and nonlinearity in combustion-acoustic interaction in diffusion flames," *J. Fluid Mech.,* Vol 594, 2008, pp. 29–57.

[6]Mitchell, C. E., Crocco, L. and Sirignano, W. A. "Nonlinear Longitudinal Instability in Rocket Motors with Concentrated Combustion," *Comb. Sci. Tech,* Vol. 1, 1969, pp. 35–64.

[7]Chu, B-T. "Analysis of a Self-Sustained Thermally Driven Nonlinear Vibration," *Phys. Fluids,* Vol. 6, No. 11, 1963, pp. 1638–1644.

[8]Culick, F. E. C. "Nonlinear Growth and Limiting Amplitude of Acoustic Oscillations in Combution Chambers," *Comb. Sci. Tech,* Vol. 3, 1971, pp. 1–16.

[9]Zinn, B. T. and Lores, M. E. "Application of the Galerkin Methods in the Solution of Nonlinear Axial Combustion Instability Problems in Liquid Rockets," *Comb. Sci. Tech,* Vol. 4, 1972, pp. 269–278.

[10]Lores, M. E. and Zinn, B. T. "Nonlinear Longitudinal Combustion Instability in Rocket Motors," *Comb. Sci. Tech,* Vol. 7, 1973, pp. 245–256.

[11]Culick, F. E. C. "Nonlinear behaviour of acoustic waves in combustion chambers - Parts I & 2," *Acta Astronautica,* Vol. 3, 1976, pp. 715–734, 735–757.

*http://www-diva.eng.cam.ac.uk/AIM_Network/AIM_home.html

[12]Awad, E. and Culick, F. E. C. "On the Existence and Stability of Limit Cycles for Longitudinal Acoustic Modes in a Combustion Chamber" *Comb. Sci. Tech,* Vol. 46 No. 3, 1986, pp. 195–222.

[13]Paparizos, L. G. and Culick, F. E. C. "The Two-mode Approximation to Nonlinear Acoustics in Combustion Chambers I. Exact Solutions for Second Order Acoustics" *Comb. Sci. Tech,* Vol. 65 No. 1, 1989, pp. 39–65.

[14]Yang, V. and Culick, F. E. C. "On the Existence and Stability of Limit Cycles for Transverse Acoustic Oscillations in a Cylindrical Combustion Chamber. 1: Standing Modes" *Comb. Sci. Tech,* Vol. 72 No. 1, 1990, pp. 37–65.

[15]Yang, V., Kim, S. I. and Culick, F. E. C. "Triggering of Longitudinal Pressure Oscillations in Combustion Chambers. I: Nonlinear Gas Dynamics" *Comb. Sci. Tech,* Vol. 72 No. 4, 1990, pp. 183–214.

[16]Lieuwen, T. C. and Yang, V. *Combustion instabilities in gas turbine engines*, AIAA, 2005.

[17]Baum, J. D., Levine, J. N. and Lovine, R. L. "Pulsed Instability in Rocket Motors: A Comparison Between Predictions and Experiment" *J. Prop. Power,* Vol. 4 No. 4, 1988, p. 308.

[18]Ananthkrishnan, N., Deo, S. and Culick, F. E. C. "Reduced-order Modeling and Dynamics of Nonlinear Acoustic Waves in a Combustion Chamber" *Comb. Sci. Tech,* Vol. 177 No. 2, 2005, pp. 221–248.

[19]Noiray, N., Durox, D., Schuller, T. and Candel, S. M. "A unified framework for nonlinear combustion instability analysis based on the flame describing function," *J. Fluid Mech.,* Vol. 615, 2008, pp. 139 - 167.

[20]Strogatz, S. H. "Nonlinear Dynamics And Chaos" *Westview Press.* 2001

[21]Sterling, J. D. "Nonlinear Analysis and Modelling of Combustion Instabilities in a Laboratory Combustor" *Comb. Sci. Tech,* Vol. 89 No. 1, 1993, pp. 167–179.

[22]Kabiraj, L., Sujith, R. I. and Wahi, P. "Experimental Studies of Bifurcations leading to Chaos in a Laboratory Scale Thermoacoustic System" *ASME Turbo Expo,* 2011, GT2011-46149.

[23]Campa, G. and Juniper, M. P. "Obtaining bifurcation diagrams with a thermoacoustic network model" *ASME Turbo Expo,* 2012, GT2012-68241.

[24]Stow, S. R. and Dowling, A. P. "Low-order Modelling of Thermoacoustic Limit Cycles" *ASME Turbo Expo,* 2004, GT2004-54245.

[25]Raleight, W. S. "The Theory of Sound Vol. 2" *Dover.* 1896

[26]Juniper, M. P. "Triggering in the horizontal Rijke tube: nonnormality, transient growth and bypass transition," *J. Fluid Mech.,* Vol. 667 2011, pp. 272-308.

[27]Subramanian, P., Mariappan, S., Sujith, R. I. and Wahi, P. "Bifurcation analysis of thermoacoustic instability in a horizontal Rijke tube," *Int. J. Spray Comb. Dyn.,* , 2011, Vol. 2 (4) pp. 325–355.

[28]Kabiraj, L. and Sujith, R. I. "Investigation of Subcritical Instability in Ducted Premixed Flames" *ASME Turbo Expo,* , 2011, GT2011-46155.

[29]Mariappan, S., Sujith, R. I. and Schmid, P. J. "Modelling nonlinear thermoacoustic instability in an electrically heated Rijke tube" *J. Fluid Mech.,* Vol. 680, 2011, pp. 511–533.

[30]Waugh, I. C., Geuss, M. and Juniper, M. P. "Triggering, bypass transition and the effect of noise on a linearly stable thermoacoustic system," *Proc. Combust. Inst.,*, Vol. 33, 2011, pp. 2945–2952.

[31]Schmid, P.J. "Nonmodal Stability Theory," *Annu. Rev. Fluid Mech.*, Vol. 39, 2007, pp. 129–162.

[32]Bewley, T. "Flow control: new challenges for a new Renaissance," *Prog. Aerospace. Sci.,* Vol. 37, 2001, pp. 21–58.

[33]Juniper, M. P. and Waugh, I. C. "Bypass Transition to Sustained Thermoacoustic Oscillations in a Linearly-stable Rijke Tube " *AIAA Aeroacoustics, KTH, Stockholm* , 2010.

[34]Juniper, M. P. "Transient growth in the horizontal Rijke tube: nonlinear optimal initial states," *Int. J. Spray Comb. Dyn.,* , 2011, Vol. 3 (3) pp. 209–224.

[35]Skufca, J. D., Yorke, J. A. and Eckhardt, B. "Edge of chaos in a parallel shear flow " *Phys. Rev. Lett.* Vol. 96, 2006, 174101.

[36]Schneider, T. M., Eckhardt, B. Yorke, J. A. "Turbulence transition and the edge of chaos in pipe flow " *Phys. Rev. Lett.* Vol. 99, 2007, 034502.

[37]Duguet, Y., Willis, A.P. & Kerswell, R.R. "Transition in pipe flow: the saddle structure on the boundary of turbulence" *J. Fluid Mech.* Vol. 613, 2008, pp. 255–274.

[38]Waugh, I. C., Geuss, M. and Juniper, M. P. "Triggering in a thermoacoustic system with stochastic noise," *Int. J. Spray Comb. Dyn.,* , 2011, Vol. 3 (3) pp. 225–242.